Modeling and Control of Fractional Order PID Controller fed Rotary Inverted Pendulum

Abhijeet Lanjewar*, *Student Member, IEEE,* Swapnil W. Khubalkar, *Student Member, IEEE,*
and Anjali S. Junghare, *Member, IEEE*
Department of Electrical Engineering,
Visvesvaraya National Institute of Technology, Nagpur, India- 440010
Email: *lanjewarabhijeet@gmail.com

***Abstract*—This paper focuses on modeling and control of rotary inverted pendulum (RIP) by using a linear quadratic regulator (LQR). The performance of the system is improved by using LQR and proportional-integral-derivative (PID) controller. Further improvement in control is obtained by using LQR and fractional-order PID (FOPID) controller. Hence, hybrid control techniques (PID+LQR and FOPID+LQR) are used to control RIP. The comparison of all the three techniques is shown. RIP is single input multiple output (SIMO) non-linear system, hence it's a challenging plant to control. So, the aim is to effectively control two output states of RIP model and the stabilization. As LQR controller takes a lot of efforts to get optimal control gain and there is a maximum deviation in the arm angle which leads to propose a hybrid controller. Simulation results show that the hybrid FOPID+LQR controller overcomes the flaw in LQR controller as well as PID+LQR controller. Controllers are analyzed based on peak overshoot, control efforts, and performance indices.**

***Index Terms*—Control Efforts, Controller Design, Fractional Calculus, Fractional-order PID (FOPID), Hybrid Controller, Inverted pendulum, Modeling, Particle Swarm Optimization (PSO)**

I. Introduction

Inverted Pendulum is broadly classified into two types i.e. cart type system and rotary type. Rotary inverted pendulum (RIP) is a complex system which involves many problems such as control, robustness, and tracking problem [1], [2]. The rotary type system is considered for investigation. RIP finds an application in missile launch pads, robotic arm, satellites, Segway-scooters, etc. RIP is highly non-linear and open loop unstable system when the pendulum is at upright position [3]. When the pendulum is at down position ($-180°$), the state is said to be stable equilibrium state and when the pendulum is at upright (vertical) position ($0°$), the state is said to be unstable equilibrium state. To design a controller for such a highly unstable system is a challenging task. To stabilize the pendulum at $0°$, many linear, non-linear, and intelligent controllers are used [4]. Linear controllers such as LQR, PID are used by linearizing the model [5]. Intelligent controllers such as fuzzy, neural are also used and compared with non-linear controllers such as sliding mode control and backstepping control [2], [6], [7].

There are three modes in which RIP can be analyzed i.e. swing-up mode, stabilization mode, and tracking control mode [8], [9]. In swing-up mode, pendulum moves from $-180°$ to $0°$ i.e. self- erected. Whereas, in stabilization mode, the pendulum is kept at $0°$ erected by hand and to stabilize at that point different control techniques are used.

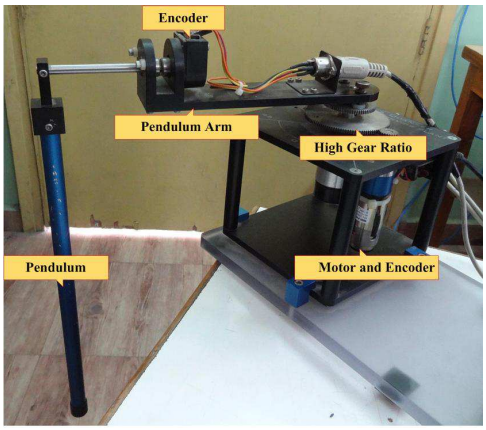

Fig. 1: Rotary inverted pendulum plant

The stabilization mode of the Quanser RIP module is considered for the study. It mainly consists of brushless DC (direct current) motor, pendulum arm, and pendulum as shown in Fig. 1 [10]. Faulhaber's brushless DC motor is used to rotate a pendulum arm which has high initial torque. The pendulum arm mounted on output gear which is driven by this motor. There are two gear ratio configurations i.e. high gear and low gear; high gear configuration with ratio 1:70 is used here. At the end of pendulum arm, the pendulum is suspended with the help of metal shaft which is built with an encoder to measure the angle. Encoder offers the resolution of 4096 counts per revolution. By encoder, position of the arm is feedback to the motor shaft. As the motor rotates clockwise or anti-clockwise, it drives the output gear with that the arm moves to control the pendulum in an upright position. With the help of data acquisition card, the RIP module is integrated which is driven by Matlab/Simulink based real-time software.

Linear quadratic regulator (LQR) is another control technique in which system dynamics are represented by linear differential equations [1], [11]. PID is a most common controller which is widely used in control [12], [13]. Further improvement in PID controller is obtained by using generalized PID controller i.e. FOPID controller [14]–[16]. In [17]–[20],

978-1-5386-2462-3/18/$31.00 ©2018 IEEE

performance of PID controller is improved by using FOPID controller. There are many optimization and optimal control techniques present in the literature for linear and non-linear dynamical systems [19]. The recent development in the area of artificial intelligence, such as fuzzy logic theory, artificial neural network, and evolutionary computational techniques such as genetic algorithm, and particle swarm optimization (PSO), etc. Commonly, all these are known as intelligent computational techniques which have given novel solutions to various control system problems [21], [22].

In this paper, the LQR, PID, and FOPID controllers are simulated and their behavior is compared. The major objectives of this paper include:

- Hybrid controller PID+LQR designed for non-linear inverted pendulum system.
- Hybrid controller PID+LQR is improved by using FOPID controller.

The contents of the paper are given as: Section 2 describes the mathematical modeling of RIP. Section 3 describes the proposed control structures. Section 4 compares simulation results of all the three strategies. Section 5 gives hardware results and paper concluded in Section 6.

II. Modeling of Rotary Inverted Pendulum (RIP)

The free body diagram of RIP is shown in Fig. 2. The system parameters are given in the Table I. The rotary arm when moves in counter-clockwise direction θ is taken as positive and for the clockwise direction, it is taken as negative, same assumption is made in the case of pendulum angle α. By employing a Lagrangian method [10], two sets of non-linear equations are obtained which can correlate with two degrees of freedom of RIP system.

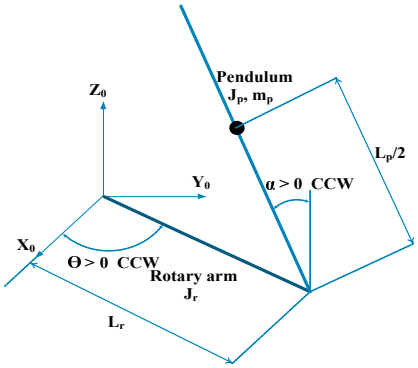

Fig. 2: Free body diagram of RIP

The Lagrangian equation can be formulated as (1).

$$L = Kinetic\ \ energy - Potential\ \ energy \tag{1}$$

For rotary arm,

$$\frac{\partial^2 L}{\partial t \partial \dot{\theta}} - \frac{\partial L}{\partial \theta} = \tau - B_r \dot{\theta} \tag{2}$$

For pendulum Arm,

$$\frac{\partial^2 L}{\partial t \partial \dot{\alpha}} - \frac{\partial L}{\partial \alpha} = \tau - B_p \dot{\alpha} \tag{3}$$

TABLE I: Parameters

Parameter	Value(units)
Rotary Arm Length (L_r)	0.2519 m
Pendulum Length (L_p)	0.3365 m
Rotary Arm Mass (m_r)	0.257 kg
Pendulum Arm Mass (m_p)	0.127 kg
Rotary Arm Moment of Inertia (J_r)	9.98e^-4 kg-m^2
Pendulum Moment of Inertia (J_p)	0.0043 kg-m^2
SRV02 System gear ratio (K_g)	70
Back EMF constant (k_m)	7.68e^-3 V/(rad/sec)
Motor Torque constant (k_t)	7.68e^-3 N-m/A
Acceleration due to gravity (g)	9.81 m/s^2
Gearbox efficiency (n_g)	0.90
Motor efficiency (n_m)	0.69
Armature Resistance (R_m)	2.6 ohm
Arm Damping coefficient (B_r)	0.0024 N.m.s/rad
Pendulum Damping coefficient (B_p)	0.0024 N.m.s/rad

Thus, the two non-linear equations of motion for RIP plant are as (4) and (5).

$$\begin{aligned}(m_p L_r^2 + \frac{1}{4} m_p L_p^2 - \frac{1}{4} m_p L_p^2 \cos^2\alpha + J_r)\ddot{\theta} - \\ (\frac{1}{2} m_p L_p L_r \cos\alpha)\ddot{\alpha} + (\frac{1}{2} m_p L_p^2 \sin\alpha\cos\alpha)\dot{\theta}\dot{\alpha} \\ +(\frac{1}{2} m_p L_p L_r \sin\alpha)\dot{\alpha}^2 = \tau - B_r\dot{\theta}\end{aligned} \tag{4}$$

$$\begin{aligned}-(\frac{1}{2} m_p L_p L_r \cos\alpha)\ddot{\theta} + (J_p + \frac{1}{4} m_p L_p^2)\ddot{\alpha} - \\ \frac{1}{4} m_p L_p^2 \cos\alpha \sin\alpha \dot{\theta}^2 - \frac{1}{2} m_p L_p g \sin\alpha = -B_p\dot{\alpha}\end{aligned} \tag{5}$$

The torque produced by servo motor is given by (6).

$$\tau = \frac{\eta_g K_g n_m k_t (V_m - K_g k_m \dot{\theta})}{R_m} \tag{6}$$

Linearize (4) and (5) with initial conditions $\theta_0 = 0, \alpha_0 = 0, \dot{\theta}_0 = 0, \dot{\alpha}_0 = 0$ to get (7) and (8).

$$(m_p L_r^2 + J_r)\ddot{\theta} - \frac{1}{2} m_p L_p L_r \ddot{\alpha} = \tau - B_r\dot{\theta} \tag{7}$$

$$-\frac{1}{2} m_p L_p L_r \ddot{\theta} + (J_p + \frac{1}{4} m_p L_p^2)\ddot{\alpha} - \frac{1}{2} m_p L_p g \alpha = -B_p\dot{\alpha} \tag{8}$$

By using above Eqs. state-space can be represented as,

$$\begin{bmatrix} \dot{\theta} \\ \dot{\alpha} \\ \ddot{\theta} \\ \ddot{\alpha} \end{bmatrix} = \begin{bmatrix} 0 & 0 & 1 & 0 \\ 0 & 0 & 0 & 1 \\ 0 & 53.10 & -0.659 & -0.658 \\ 0 & 98.38 & -0.658 & -1.218 \end{bmatrix} \begin{bmatrix} \theta \\ \alpha \\ \dot{\theta} \\ \dot{\alpha} \end{bmatrix} + \begin{bmatrix} 0 \\ 0 \\ 274.40 \\ 273.96 \end{bmatrix} V_o; \tag{9}$$

$$y = \begin{bmatrix} 1 & 0 & 0 & 0 \\ 0 & 1 & 0 & 1 \end{bmatrix} \begin{bmatrix} \theta \\ \alpha \\ \dot{\theta} \\ \dot{\alpha} \end{bmatrix} \tag{10}$$

III. Control Scheme and Proposed Controllers

Basic block diagram of hybrid control scheme is shown in Fig. 3. In place of controller 1, PID or FOPID controller is used, while controller 2 is always considered to be LQR. Here, three control schemes have considered for the optimal control of RIP system: 1) with LQR control method. 2) LQR with one rotary arm PID (Hybrid) control method. 3) LQR with one rotary arm FOPID (Hybrid) control method.

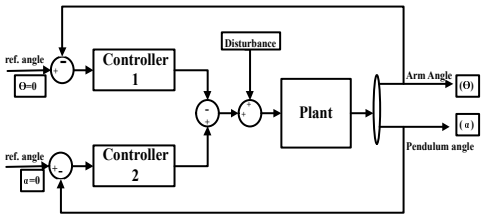

Fig. 3: Basic block diagram of the RIP control system

A. LQR Controller

Optimal control can be done using LQR method. In this method, it takes system state dynamics i.e. $(\theta, \alpha, \dot{\theta}, \dot{\alpha})$ with control input as feedback to make the system sane and sensible. In mathematical modelling as given in Section 2, the non-linear equations of RIP system have linearized at upright (unstable equilibrium) point with initial condition $x_0 = [0\ 0\ 0\ 0]^T$. LQR is designed with the help of linear state-space model. Linear state-space equation is given by (11).

$$\dot{x} = Ax + Bu \tag{11}$$

where, $x = [\theta, \alpha, \dot{\theta}, \dot{\alpha}]^T$. State variable feedback control is given as $u = -Kx$ which leads to (12).

$$\dot{x} = (A - K)x + Bu \tag{12}$$

where, K is LQR gain vector i.e. $K = R^{-1}B^TP$. This K directly relates with the minimized cost function (13).

$$J = \int (X^TQX + u^TRu)dt \tag{13}$$

where, Q and R define the system error and the control effort (u) respectively which are entitled to weighting matrices. P is positive definite symmetric constant matrix obtained from algebraic Reccatti equation (14).

$$A^TP + PA - PBR^{-1}B^TP + Q = 0 \tag{14}$$

As θ and α are needed to be settled in good time. So, weighting matrices are considered as (15).

$$Q = \begin{bmatrix} 1 & 0 & 0 & 0 \\ 0 & 100 & 0 & 0 \\ 0 & 0 & 0 & 0 \\ 0 & 0 & 0 & 0 \end{bmatrix}; R = [10] \tag{15}$$

This gives optimal state feedback control gain $K = [-0.3162\ \ 4.2655\ \ -0.2356\ \ 0.4106]$.

B. PID Controller

PID controller handles the error of the system. Error $e(t)$ in the system is changing over the time. In the proportional path, the error is scaled by gain K_p. When the error is large, the proportional path will produce a large output and when the error is zero the output in proportional path is zero and when it is negative the output is negative. In integral path, as the error moves over time, the integral will continue to sum it up and multiplied by constant K_i. Integral path is used to remove constant error in the system no matter how small the error will be eventually the summation of that error will be significant enough to adjust the controller output. When the change in signal is moving relatively slow, the derivative path (K_d) is small and faster the error changes, the larger the derivative path. By summing up these three paths, PID controller (16) is achieved [13].

$$u(t) = K_pe(t) + K_i \int e(t) + K_d \frac{d}{dt}e(t) \tag{16}$$

where $u(t)$ is control signal.

C. Hybrid: PID+LQR Controller

This hybrid controller came because of dilemma of choosing the constants of LQR controller and sluggish response in rotary arm angle. Exact weighting matrices for the non-linear system is much difficult task. In the control scheme as shown in Fig. 3, both PID and LQR controllers are used to stable the arm at the reference and the pendulum at an upright position. In LQR, all the 4 states are feedback with optimal control gain, in addition to that PID controller is added. PID controller is used for rotary arm angle (θ) because in LQR control method variation in arm angle is more predominant. The equation of the PID controller for rotary arm angle is given as (17).

$$u(t) = K_pe_\theta(t) + K_i \int e_\theta(t) + K_d \frac{d}{dt}e_\theta(t) \tag{17}$$

where, $e_\theta(t)$ is arm angle error.

D. FOPID

FOPID controller is proposed in place of PID controller for performance improvement. In FOPID, in addition to K_p, K_i, and K_d, two more parameters (λ - order of integrator, μ - order of differentiator) are available that give extra chance for the improvement in the controller. The FOPID controller is described by the fractional-order differential equation (18).

$$u(t) = K_pe(t) + K_iD^{-\lambda}e(t) + K_dD^{\mu}e(t) \tag{18}$$

Applying Laplace transform, the transfer function of the controller can be expressed by (19).

$$u(s) = K_p + K_is^{-\lambda} + K_ds^{\mu}, (\lambda, \mu > 0) \tag{19}$$

Any ratio of rational transfer function is characterized by its poles and zeros [14]- [20]. The Bode magnitude plot of the fractional-order transfer function has slope of $\pm\lambda 20dB/dec$ and the Bode phase plot is constant at value equal to $\pm\lambda 90°$. This is obtained by interlacing real poles and zeros [16]. Hence, the integer order approximation is achieved within the desired frequency band(ω_l, ω_h) using Oustaloup et al. approximation method [23]. Here, poles and zeros are obtained as follows (20):

$$D_N(s) = \left(\frac{\omega_u}{\omega_h}\right)^{\alpha} \Pi_{k=-N}^{N} \left(\frac{1 + s/\omega_k'}{1 + s/\omega_k}\right) \tag{20}$$

where, $\omega_k = \omega_b \left(\frac{\omega_h}{\omega_b}\right)^{\left(\frac{(k+N+1/2+\alpha/2)}{(2N+1)}\right)}$

$\omega_{k'} = \omega_b \left(\frac{\omega_h}{\omega_b}\right)^{\left(\frac{k+N+1/2-\alpha/2}{(2N+1)}\right)}$

The number of zeros or poles are given as 2N+1, the approximation order (N) is considered as 3.

E. Proposed FOPID+LQR Controller

Same as that of PID+LQR, FOPID+LQR is proposed due to advantages of FOPID over PID control. FOPID is used as controller 1 in Fig. 3 while LQR is used as controller 2. The equation of the FOPID controller used for rotary arm angle is given as (21).

$$u(t) = K_p e_\theta(t) + K_i D^{-\lambda} e_\theta(t) + K_d D^{\mu} e_\theta(t) \tag{21}$$

F. Optimization of Controller Parameters

Recently, many researchers have focused on controllers tuning and obtained meaningful results [24]. In this work, dynamic particle swarm optimization (DPSO) method is used to tune the controller parameters. Here, each particle in swarm represents a solution to the problem defined by its instantaneous position and velocity [25]. DPSO is an improvement in PSO obtained by adding the product of differences in objective function value between a particle, the individual best, or the global best. Here, the change in position of a particle is directly proportional to iteration, which further depends on individual best, global best, and a random velocity [21], [26]. In DPSO, the new velocity of a particle is obtained by (22):

$$\begin{aligned} v_{id} = (f(p_{id}) - f(x_{id})) \times (p_{id} - x_{id}) \times sf_1 + \\ (f(p_{gd}) - f(x_{id})) \times (p_{gd} - x_{id}) \times sf_2 + \\ randm() \times signis() \times sf_3 \end{aligned} \tag{22}$$

where, p_{id}: individual best, p_{gd}: global best, v_{id}: velocity of a particle, x_{id}: current position of a particle, sf_1, sf_2, sf_3: to scale the calculated value in the range of the control variable, $randm$: random function, $signis$: function which generates random positive or negative value. Maximum iteration is set as 50, population size is taken as 100, lower and higher translation frequencies are considered as $\omega_l = 0.1$ rad/s and $\omega_h = 1000$ rad/s. ITAE (integral time absolute error) is chosen as performance criterion [22]. The values of controller parameters, obtained from DPSO, are implemented in PID and FOPID controllers in simulation. The optimized values of the controllers are presented in Table II.

TABLE II: Optimized Gain and Order Values

Controllers with LQR	K_p	K_i	K_d	λ	μ
PID	0.54	0.028	0.0357	1	1
FOPID	0.611	0.052	0.048	0.74	0.767

IV. Simulation Results and Discussion

A. Design

Matlab/Simulink is used for simulation. Model for the analysis of RIP is shown in Fig. 4. Reference arm angle (θ) and the pendulum angle (α) are set to 0°(stabilization mode). Pulse generator and band limited white noise is used as disturbance. All the three strategies, as discussed in Section 3, are checked and the results are presented.

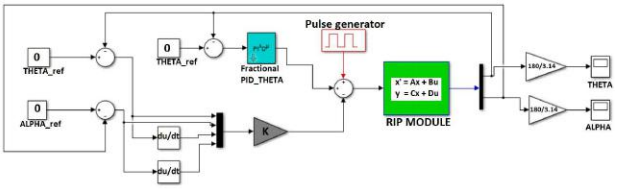

Fig. 4: Matlab/Simulink model of the RIP control system

B. Results and Discussion

1) with Pulse Generator as Disturbance: The responses obtained for LQR, PID+LQR, and FOPID+LQR with pulse generator are shown here. Pulse generator with an amplitude of 1.2 is applied as a disturbance to the system. Rotary arm shows a slow response with LQR controller as shown in Fig. 5 with peak overshoot of 10°. This slow response of rotary arm angle leads to use a PID+LQR controller. As PID+LQR controller reduces the peak overshoot of arm and pendulum angle as shown in Fig. 5, FOPID+LQR is considered for further improvement. Analysis of Fig. 5 is tabulated in Table III.

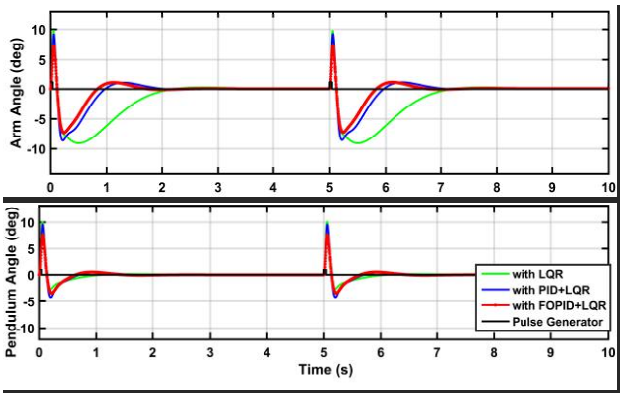

Fig. 5: Responses of arm angle θ and pendulum angle α

TABLE III: Maximum Absolute Values for Different Controllers

Controllers	LQR	PID+LQR	FOPID+LQR
Alpha(deg)	10	9	6.5
Theta(deg)	10	8.5	7
Control signal (v)	1.4	1.1	0.82

Error in arm angle and pendulum angle are shown in Figs. 6 and 7 respectively. The error signal in arm angle θ reaches to its minimum value and in minimum time of 1.7 s with proposed FOPID+LQR controller. The error signal analysis for Figs. 6 and 7 is tabulated in Table IV and V respectively. It is observed that the performance indices (PI) i.e. integral absolute error(IAE), integral square error (ISE), and integral time absolute error (ITAE) is less in the case of FOPID+LQR controller.

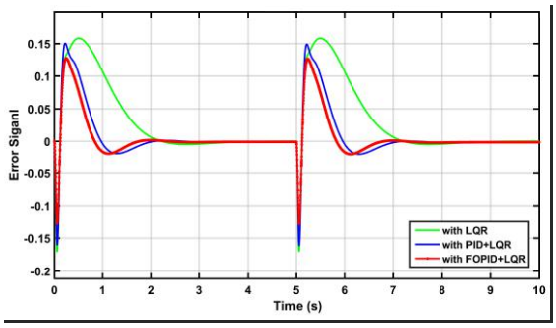

Fig. 6: Error signal in arm angle θ of RIP system

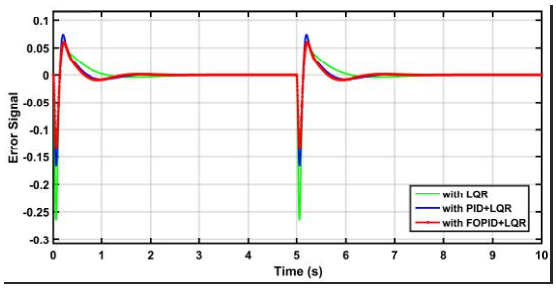

Fig. 7: Error signal in pendulum angle α of RIP system

TABLE IV: Analysis of Error in Arm Angle θ

PI	LQR	PID+LQR	FOPID+LQR
IAE	0.3667	0.1889	0.1443
ISE	0.0425	0.0175	0.0111
ITAE	1.1211	0.6009	0.4600

TABLE V: Analysis of Error in Pendulum Angle α

PI	LQR	PID+LQR	FOPID+LQR
IAE	0.0605	0.0590	0.0574
ISE	0.0039	0.0035	0.0030
ITAE	0.1768	0.1710	0.1657

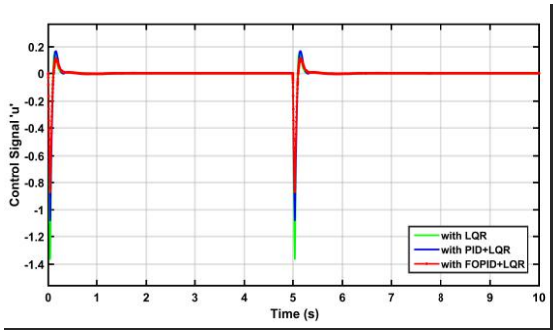

Fig. 8: Control signal 'u' of RIP system

Control efforts (u) of the controller are shown in Fig. 8 and quantified in Table VI. The control signal is bounded in the range of [-1.4 to 0.2] for LQR controller, whereas, the control range is further reduced to [-0.85 to 0.13] with proposed FOPID+LQR controller. Control efforts are quantified using performance indices integral absolute control effort (IACE), integral square control effort (ISCE), and integral time absolute control effort (ITACE).

TABLE VI: Control Effort Analysis

PI	LQR	PID+LQR	FOPID+LQR
IACE	0.1598	0.1476	0.1173
ISCE	0.1211	0.0831	0.0521
ITACE	0.4153	0.3856	0.3574

2) with White Noise as Disturbance: Controllers are tested with band limited white noise as disturbance of noise power 0.015 to compare the robustness with one another. Fig. 9 shows the response of arm and pendulum angle with white noise for all the three strategies. Variation in arm angle is $+15^\circ$ to -20° for FOPID+LQR controller which reduces from $\pm 45^\circ$ in LQR. Deviation in pendulum angle is also less in proposed FOPID+LQR as compared to other two controllers. Its analysis is tabulated in Table VII.

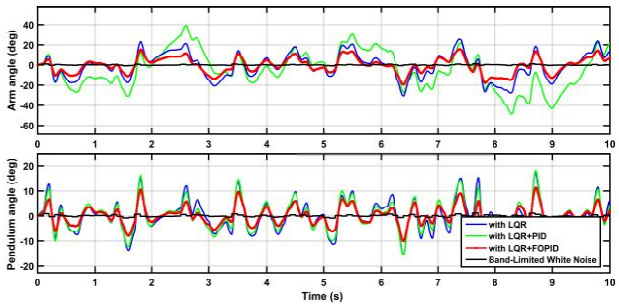

Fig. 9: Responses of arm angle θ and pendulum angle α

TABLE VII: Maximum Absolute Values for Different Controllers

Controllers	LQR	PID+LQR	FOPID+LQR
Alpha(deg)	18	17	11
Theta(deg)	45	26	17
Control signal (v)	1.25	0.8	0.5

Error in arm and pendulum angle are curtailed by using proposed hybrid controller as referring to Fig. 10 and Fig. 11 respectively. Its analysis is quantified in Table VIII and IX respectively. Control effort (u) of controllers, with white noise, is shown in Fig. 12, which is less in the case of proposed FOPID+LQR controller. Control effort analysis, with white noise, is tabulated in Table X.

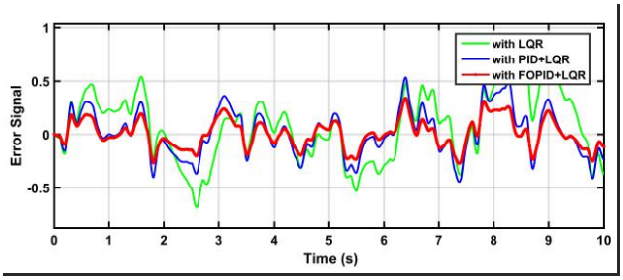

Fig. 10: Error signal in arm angle θ of RIP system

TABLE VIII: Analysis of Error in Arm Angle θ

PI	LQR	PID+LQR	FOPID+LQR
IAE	2.757	1.707	1.058
ISE	1.092	0.4475	0.2536
ITAE	15.13	9.154	5.636

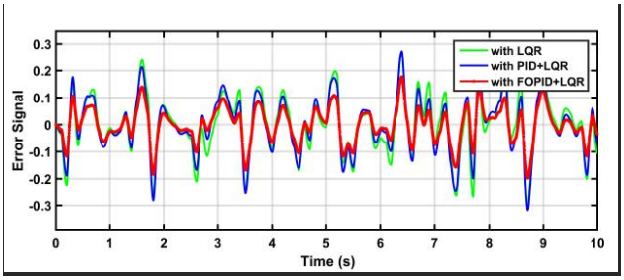

Fig. 11: Error signal in pendulum angle α of RIP system

TABLE IX: Analysis of Error in Pendulum Angle α

PI	LQR	PID+LQR	FOPID+LQR
IAE	0.8149	0.7764	0.5040
ISE	0.1018	0.0985	0.04142
ITAE	4.1640	3.9872	2.5911

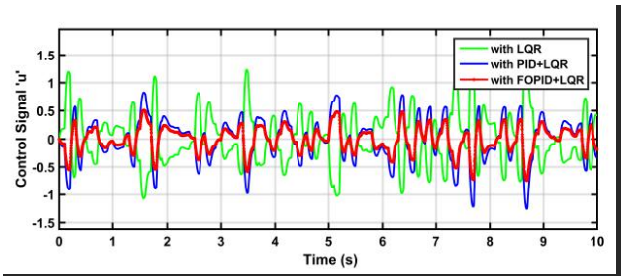

Fig. 12: Control signal 'u' of RIP system

TABLE X: Control Effort Analysis

PI	LQR	PID+LQR	FOPID+LQR
IACE	3.823	2.909	1.7710
ISCE	2.3810	1.3810	0.8103
ITACE	19.661	14.930	9.078

V. Conclusion

In this paper, modeling and control of rotary inverted pendulum with new hybrid controller are presented to overcome the drawbacks in LQR controller. By selecting FOPID controller with LQR, an edge over PID+LQR controller is achieved. By comparing the results of three controllers, it is observed that FOPID+LQR controller gives a clear advantage over other controllers. Peak overshoot and steady state oscillation in rotational arm angle and pendulum angle are reduced with proposed FOPID+LQR control strategy. The control efforts required in case of FOPID+LQR control strategy are minimized than other two control strategies which points towards the energy efficient nature of the controller.

Acknowledgement

Support provided by the Board of Research of Nuclear sciences, India, under the project sanction no. BRNS 2012/36/69-2951

References

[1] N. Muskinja and B. Tovornik, "Swinging up and stabilization of a real inverted pendulum," *IEEE Trans. on Industrial Electronics*, vol. 5 , no. 2, pp. 631-639,2006.

[2] C.W. Anderson, "Learning to control an inverted pendulum using neural networks," *IEEE Control Systems Magazine*, vol. 9, pp. 31-37, 1989.

[3] V. Casanova, J. Alcaina, J. Salt, R. Piza, and A. Cuenca, "Control of the rotary inverted pendulum through threshold-based communication," *ISA Trans.*, vol. 62, pp. 357-366, 2016.

[4] O. Boubaker, "The inverted pendulum benchmark in nonlinear control theory: a survey," *Int J of Advanced Robotic Systems*, vol. 10, no. 5, pp. 1-9, 2013.

[5] I.A. Raptis and K.P. Valavanis, *Linear and Nonlinear Control of Small-Scale Unmanned Helicopters*, Intelligent Systems, Control and Automation: Science and Engineering 45, Springer, 2011.

[6] L.X. Wang, "Stable adaptive fuzzy controllers with application to inverted pendulum tracking," *IEEE Trans. on Systems, Man, and Cybernetics, Part B (Cybernetics)*, vol. 26, no. 5, pp. 677-691,1996.

[7] A. Kisku, *Sliding Mode Control of Inverted Pendulum*, MTech Dissertation, Jadavpur University, Kolkata, 2012.

[8] K. Furuta , M. Yamakita , and S. Kobayashi, "Swing-up control of inverted pendulum using pseudo-state feedback," *Proc. of the Institution of Mechanical Engineers, Part I: Journal of Systems and Control Engineering*, vol. 206, no. 4, pp. 263-269, 1992.

[9] T. Yamakawa, "Stabilization of an inverted pendulum by a high-speed fuzzy logic controller hardware system," *Fuzzy sets and Systems*, vol. 32, no. 2, pp. 161-180, 1989.

[10] Quanser User Manual SRV02. Inverted Pendulum.

[11] L.B. Prasad, B. Tyagi, and H.O. Gupta, "Optimal control of nonlinear inverted pendulum system using PID controller and LQR: performance analysis without and with disturbance input," *Int. J. of Automation and Computing*, vol. 11, no. 6, pp. 661-670, 2014.

[12] K.J. Astrom and T. Hagglund, "The future of PID control," *Control Eng Practice*, vol. 9, no. 11, pp. 1163-1175, 2001.

[13] K.J. Astrom and T. Hagglund, *Advanced PID control*, ISA-The Instrumentation, Systems and Automation Society, 2006.

[14] K. Oldham and J. Spanier, *The Fractional Calculus*, Elsevier, 1974.

[15] I. Podlubny, "Fractional-order systems and $PI^{\lambda}D^{\mu}$controllers," *IEEE Trans. on Autom. Control*, vol. 44, no. 4, pp. 208-214, 1999.

[16] S. Das, *Functional Fractional Calculus*, Springer, NY, 2011.

[17] S. Khubalkar, A. Chopade, A. Junghare, M. Aware, and S. Das, "Design and realization of stand-alone digital fractional order PID controller for buck converter fed DC motor," *Circuits Syst. and Signal Process.*, vol. 35, no. 6, pp. 2189-2211, 2016.

[18] M.V. Aware, A.S. Junghare, S.W. Khubalkar, A. Dhabale, S. Das, and R. Dive, "Design of new practical phase shaping circuit using optimal polezero interlacing algorithm for fractional order PID controller," *Analog Integr. Circuits and Signal Process.*, pp. 1-15, 2017.

[19] A.S. Chopade, S.W. Khubalkar, A.S. Junghare, M.V. Aware, and S. Das, "Design and implementation of digital fractional order PID controller using optimal pole-zero approximation method for magnetic levitation system," *IEEE/CAA J. of Automatica Sinica*, pp. 1-12, 2016.

[20] I. Petras, "Fractional-order feedback control of a DC motor," *J. of Electrical Engineering*, vol. 60, no. 3, pp. 117-128,2009.

[21] A. Badar, B.S. Umre, and A.S. Junghare, "Reactive power control using dynamic particle swarm optimization for real power loss minimization," *Electrical Power and Energy Systems*, vol. 41, pp. 133-6, 2012.

[22] W. Zheng , Y. Pi "Study of the fractional order proportional integral controller for the permanent magnet synchronous motor based on the differential evolution algorithm," *ISA Trans.*, vol. 63, pp. 387-393,2016.

[23] A. Oustaloup, F. Levron, B. Mathieu, and F. Nanot, "Frequency-band complex noninteger differentiator- characterization and synthesis," *IEEE T. Circuits I*, vol. 47, pp. 25-39, 2000.

[24] F. Padula and A. Visioli, "Optimal tuning rules for proportional-integral-derivative and fractional-order proportional-integral-derivative controllers for integral and unstable processes," *IET Control Theory Applications*, vol. 6, no. 6, pp. 776-786, 2012.

[25] R. Song and Z. Chen, "Design of PID controller for maglev system based on an improved PSO with mixed inertia weight," *J. of Networks*, vol. 9, no. 6, pp. 1509-1517, 2014.

[26] S.W. Khubalkar, A.S. Junghare, M.V. Aware, A.S. Chopade, and S. Das, "Demonstrative fractional order - PID controller based DC motor drive on digital platform," *ISA Trans.*, pp. 1-15, 2017.